Neonlike iron x-ray laser: Population kinetics and radiative transfer

D. Benredjem, P. Zeitoun, A. Sureau, and C. Möller
Laboratoire de Spectroscopie Atomique et Ionique, Université Paris–Sud, Centre d'Orsay, Bâtiment 350, 91405 Orsay Cedex, France
(Received 15 May 2000; published 24 April 2001)

In this work, we present collisional-radiative calculations for neonlike iron x-ray lasers. These calculations show the importance of the interaction between the x-ray laser beam and the amplifying medium, which is taken into account in the paraxial Maxwell-Bloch approach. Our calculations are in better agreement with a recent experiment (a prepulse plus two main pulses) on the $3p$-$3s$ 0–1 line, than the code EHYBRID which ignores the above interaction. Saturation is attained for plasma lengths near 1 cm, and the calculated effective gain agrees with the experimental value, at least for the first main pulse.

DOI: 10.1103/PhysRevE.63.056407 PACS number(s): 52.25.Dg, 42.55.Vc, 32.80.−t

I. INTRODUCTION

Soft-x-ray amplification has been demonstrated in neonlike ions [1,2] and nickel-like ions [3–5] in the collisional excitation scheme. Recent progress has also been made in the recombination scheme [6]. Strong amplification in the collisional excitation scheme has been demonstrated for wavelengths ranging from 84.7 nm in Si [7] to 3.5 nm in Au [8]. In capillary-discharge systems, gain-length products greater than 25 have been obtained at 46.9 nm in Ar by Rocca *et al.* using double pass amplification [9]. Saturation has been reported in neon-like Zn [2], Ge [10,11], Se [8], and Y [12], and in nickel-like Ag [5] and Pd [13].

Population inversions can be obtained for the transitions $(2p^5j_1,3pj_2)J\rightarrow(2p^5j_1,3s1/2)J'$ in neonlike ions (see Fig. 1), the strongest of which are generally $(1/2,1/2)0 \rightarrow(1/2,1/2)1$ and $(1/2,3/2)2\rightarrow(1/2,1/2)1$, referred to below as 0–1 and 2–1. The $J=0$ level cannot decay by radiative transition to the ground state, while the $J=2$ levels can, but only through electric-quadrupole transition. The levels involved in lasing are strongly populated by electron collisions (mainly from the ground state), and inversions can occur due to the fast radiative decay of the lower level.

The main objective of this work is to provide reliable results for large amplification of a neonlike iron x-ray laser (XRL) beam. For this reason, we account for the interaction of the XRL beam with the amplifying medium, in the population equations. This is done through a paraxial Maxwell-Bloch (MB) approach. Experiments on iron [14,15] have shown an important enhancement of 0–1.

This paper is twofold. In the first part, we model the experiment of Zeitoun *et al.* [14]. The hydrodynamic quantities of interest are provided by the time dependent, Lagrangian hydrocode EHYBRID [16] which considers the single-sided illumination of a slab target. This hydrodynamic code is one dimensional (1D) along the driving laser axis, and 0D (no thermal conduction, one cell) along the two other axes which are parallel to the target surface. The plasma is typically divided into 98 Lagrangian cells in the direction parallel to the heating laser; its expansion in the transverse dimension is assumed to be self-similar, each cell being considered isothermal. The incoming laser energy is absorbed by inverse Bremsstrahlung and resonant absorption at the critical surface. The rates contained in the population equations involve all significant interlevel terms, and have yielded a very satisfactory description of the laser in the small-signal regime [17].

The second part of this paper studies the line propagation of the XRL beam. In the saturation regime, one cannot treat the population kinetics and the line transfer separately. In fact, for such intensities, the XRL beam has an effect on the level populations. Moreover, the x-ray beam is amplified in one direction (the z direction); the π-polarized component is then absent. As a consequence, the level degeneracy must be explicitly considered to take into account the specific interaction of the amplified radiation with each Zeeman sublevel. The MB theory is the most appropriate approach to account for such an interaction. The combination of the Maxwell wave equation and the Bloch equations provides a set of equations that govern the evolution of Zeeman sublevels populations. A number of works have already used the MB formalism in specific investigations, such as superfluorescence [18], superradiance theory [19], gain [20], buildup of radiation [21], and transverse coherence [22].

II. SIMULATIONS WITHOUT LINE PROPAGATION

We have run a set of simulations with the aim of investigating the range of confidence of EHYBRID. Experiment versus modeling is of great importance for forthcoming studies on x-ray laser cavities, since simulations would be extensively used for the cavity design. The simulations have been tested on driving laser configurations as close as possible to the experimental conditions. We will briefly discuss the numerical results, concentrating our attention on the ability of the code to model an experiment for which prepulses have been used. In the experiment of Zeitoun *et al.* [14], a 2-cm-long flat slab target was irradiated by superimposing the six beams of the LULI facility onto a 22 mm$\times$100 μm focal line. The driving laser is composed of two Gaussian pulses of 130-ps duration (full width at half maximum) preceded by a prepulse.

In the modeling with EHYBRID, a full set of atomic data consisting of the 27 levels of Fig. 1, the ten levels that arise when the $2s$ shell is open, and two $4s$ levels, i.e., 39 levels, is used for the neonlike ion stage. Na-like and F-like ion stages are considered with a restricted number of levels which allows a correct description of the processes linked in

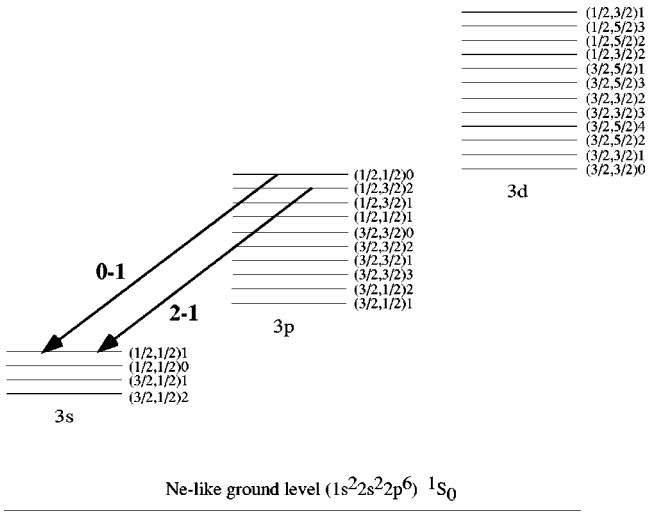

FIG. 1. Energy diagram (not to scale) of the first 27 neonlike levels arising from the configurations $1s^2 2s^2 2p^6$ (ground level) and $1s^2 2s^2 2p^5 3l$ ($l=0-2$), in j-j coupling. The levels are labeled $(j_1, j_2)J$, where j_1 and j_2 are the angular momenta of the $2p$ and $3l$ electrons, respectively. J designates the total angular momentum. The lasing lines 0-1 and 2-1 are represented.

or out of the neonlike ion. The ionization is described by Griem's model [23]. A flux limitor of 0.1 was used, and the reflectivity at critical density was set to 0.8. The intensity of each pulse has been carefully chosen in order to fit the experimental value. The prepulse is of low intensity (10^9 W/cm^2) and the two main pulses, separated by a 800 ps time interval, are of high intensity (2×10^{13} W/cm^2). The first main pulse arrives 5.6 ns after the prepulse.

The electron density and electron and ion temperatures, at the time of peak gain, are presented in Fig. 2. At this stage, the gains are local, which means that no XRL propagation along the plasma column has been taken into account in the set of collisional-radiative equations. The first important result is that for the 0–1 line the calculated gain is much larger than the measured one for the two main pulses. In fact, the calculated peak gain is 20.4 cm^{-1} for the first main pulse and 32.1 cm^{-1} for the second one, while the experimental gains are 15 and 12 cm^{-1}, respectively (see Table I). It is worth stressing that the (local) gain predicted by EHYBRID is deduced from a population inversion, while the experimental gain is obtained by fitting the measured intensity with Linford *et al.*'s formula [24].

At least two effects, not taken into account in the EHYBRID code, contribute to the above discrepancies. The first one is the XRL beam refraction which is due to a density gradient [25]. This effect is known to reduce the gain. The second effect is the interaction between the XRL beam and the plasma, which takes place at saturation. It is easy to show that this interaction reduces the gain by decreasing the population of the upper level and increasing that of the lower level. A better agreement between the calculated and measured intensity is expected if this interaction is taken into account in the collisional-radiative equations.

Finally, an experimental study [26] has demonstrated that with a driving laser of low intensity (typically below

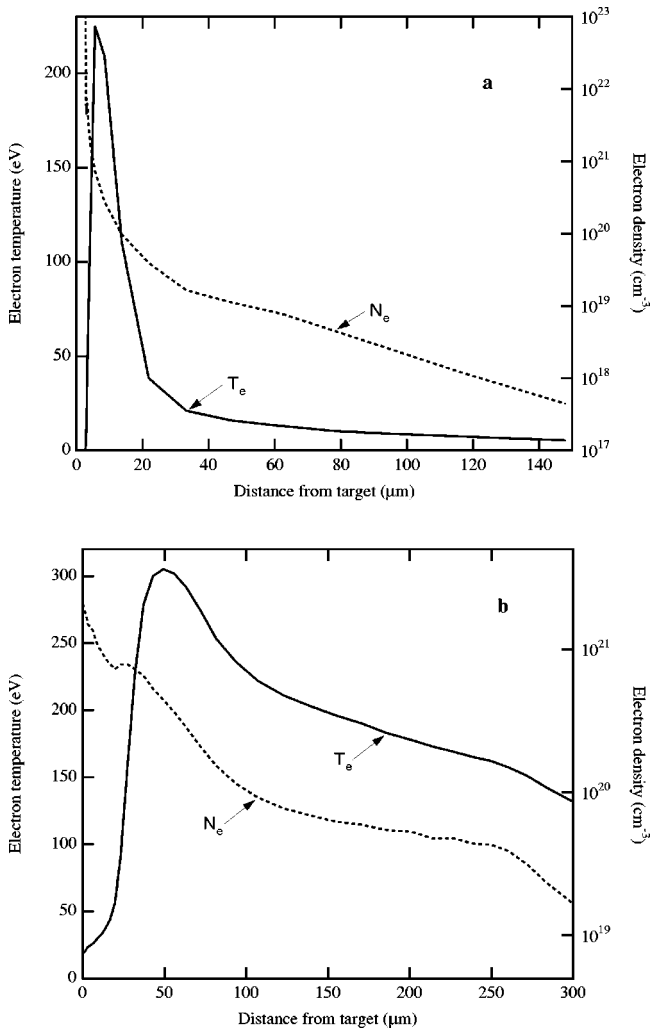

FIG. 2. Electron density and electron and ion temperatures as a function of the distance to the target surface, at the time of peak gain for the first (a) and second (b) main pulses. The experiment of Zeitoun *et al.* is modeled by using the EHYBRID code.

10^{10} W c m^{-2}), the laser-matter interaction could not be described by a pure hydrocode such as our version of EHYBRID. At these intensities, the solid state physics (thermal conductivity in solid, liquid or gas, phase transition, etc.) plays an important role in the laser-matter interaction, and must be included in the simulation. To our knowledge, the very large majority of the existing XRL codes do not take into account solid state physics.

TABLE I. Local gain (EHYBRID code) and effective gain (Maxwell-Bloch routine and experiment) of the 0–1 line in cm^{-1}. The results are obtained in the conditions of the experiment of Zeitoun *et al.*

	First pulse	Second pulse
EHYBRID	20.4	32.1
MB	12.8	17.1
Experiment	15.0	12.0

III. POPULATION KINETICS AND RADIATIVE TRANSFER PROBLEM

When the intensity of the x-ray beam is large (gain-length product $\geqslant 15$), the absorption and induced emission between the lasing levels have important effects on the population of these levels. For this reason, we perform a collisional-radiative calculation where the two processes are taken into account. A consistent approach is to use the MB formalism [27].

The time-dependent monochromatic intensity of a radiation propagating along a direction, say z, is a solution of the radiative transfer equation,

$$\frac{\partial}{\partial z} I(\nu,z,t) = j(\nu,z,t) + G(\nu,z,t) I(\nu,z,t), \tag{1}$$

where j and G are the emissivity and the local gain, respectively. The propagation of a radiation through a globally neutral plasma obeys the Maxwell wave equation

$$\Delta \mathbf{E} - \frac{1}{c^2}\frac{\partial^2}{\partial t^2}\mathbf{E} - \frac{\omega_{pe}^2}{c^2}\mathbf{E} = \frac{1}{\varepsilon_0 c^2}\frac{\partial^2}{\partial t^2}\mathbf{P}, \tag{2}$$

where $\mathbf{E}$ is the electric field, $\mathbf{P}$ the polarization vector of the plasma, and ω_{pe} the electron plasma frequency. We choose an orthonormal basis such that the x axis is perpendicular to the target surface, or, what amounts to the same thing, parallel to the direction of the driving laser. The z axis is taken parallel to the direction of the XRL beam. In this case, amplified waves do not contain the π-polarized component, and can be expressed on σ_+ and σ_- circularly polarized components only. The electric fields associated with these components can be written in the forms

$$\mathbf{E}_{\sigma+} = E\cos(\omega t - kz + \varphi_+)\mathbf{e}_x + E\sin(\omega t - kz + \varphi_+)\mathbf{e}_y, \tag{3}$$

$$\mathbf{E}_{\sigma-} = -E\cos(\omega t - kz + \varphi_-)\mathbf{e}_x + E\sin(\omega t - kz + \varphi_-)\mathbf{e}_y, \tag{4}$$

where $k=\omega/c$ is the wave vector, and $\mathbf{e}_x$ and $\mathbf{e}_y$ are unit vectors. They have the same amplitude because the spontaneous emission probability is the same for both components. A useful relation between these fields and the $\Delta M = M - M'$ values (M and M' being the magnetic quantum numbers of the upper and lower level of the lasing transition, respectively) can be established if these fields are expressed in a tensorial form. In fact, we can show that

$$\mathbf{E}_{\sigma+} = E'\{\exp[i(\omega t - kz + \varphi_+)]\mathbf{e}_1 - \exp[-i(\omega t - kz + \varphi_+)]\mathbf{e}_{-1}\}, \tag{5}$$

$$\mathbf{E}_{\sigma-} = E'\{-\exp[-i(\omega t - kz + \varphi_-)]\mathbf{e}_1 + \exp[i(\omega t - kz + \varphi_-)]\mathbf{e}_{-1}\}, \tag{6}$$

where $\mathbf{e}_{\pm 1}[=(\mp\mathbf{e}_x + i\mathbf{e}_y)/\sqrt{2}]$ are unit vectors associated with $\Delta M = \pm 1$ transitions, and where we have set $E' = -E/\sqrt{2}$.

A univocal correspondence exists between the polarization labels σ_+ and σ_-, on the one hand, and the ΔM $(=q)$ values, on the other hand. We have $\sigma_+ \Leftrightarrow q=1$, and $\sigma_- \Leftrightarrow q=-1$, and we shall hereafter label the various quantities associated with a circularly polarized wave by the value of the corresponding q. For example, the intensity $I_{\sigma^\pm}$ is noted $I^{(\pm 1)}$, and the total monochromatic intensity reads

$$I(\nu,z,t) = I^{(1)}(\nu,z,t) + I^{(-1)}(\nu,z,t). \tag{7}$$

The intensity $I^{(q)}(\nu,z,t)$ is solution of the radiative transfer equation [Eq. (1)], where the emissivity and the gain involve only $\Delta M = q$ transitions. The emissivity corresponds to the fraction of radiation spontaneously generated in a small solid angle θ centered on the z axis. It involves all the transitions $JM \rightarrow J'M'$, such that $M = M' + q$, and can be written

$$j^{(q)}(\nu,z,t) = \frac{3\theta}{8\pi}(2J+1)Ah\nu\Phi(\nu)\sum_M N_{JM}(z,t) \times \begin{pmatrix} J & 1 & J' \\ -M & q & M-q \end{pmatrix}^2, \tag{8}$$

where A is the rate of spontaneous emission from the upper lasing level J to the lower lasing level J'. Φ is the line shape function, and the N_{JM}'s designate the population densities of the Zeeman sublevels associated with the upper lasing level. The local gain is written as [28]

$$G^{(q)}(\nu,z,t) = \frac{k}{2\varepsilon_0\hbar}\Phi(\nu)\sum_M [N_{JM}(z,t) - N_{J'M-q}(z,t)] \times \langle JM|d_q|J'M-q\rangle^2, \tag{9}$$

where the d_q's are the tensorial components of the electric-dipole operator.

The radiative transfer problem is solved by partitioning the plasma column into a succession of m adjacent cylinders with a common axis z, and lengths $z_p - z_{p-1}$ $(p = 1,2,\ldots,m)$. $z_m - z_0$ is the propagation length of the x-ray beam. The intervals are chosen sufficiently small so that the populations, and then the gain and the emissivity, do not depend on z in each cylinder. The equation of transfer is then easily integrated, yielding, for $z \in [z_{p-1}, z_p]$,

$$I^{(q)}(z) = \frac{j^{(q)}(z_p)}{G^{(q)}(z_p)}\{\exp[G^{(q)}(z_p)(z - z_{p-1})] - 1\} + I^{(q)}(z_{p-1})\exp[G^{(q)}(z_p)(z - z_{p-1})], \tag{10}$$

where frequency and time are omitted. The first contribution on the right-hand side of the above equation is due to the emission spontaneously generated and amplified in the considered interval, while the second one describes the amplification, in the same interval, of the radiation coming from the preceding segment, i.e., $[z_{p-2}, z_{p-1}]$.

The radiative transfer equation must be coupled to the set of population equations. In fact, we have two groups of levels. The first one includes all neonlike ion levels except the

lasing levels. To first order, these levels are insensitive to the XRL beam, and the corresponding population equations do not contain an explicit dependence on the intensity of the XRL beam. The remaining levels, i.e., the lasing levels J and J', involve many elementary lasing transitions between the Zeeman sublevels (JM) and $(J'M')$, where $-J \leqslant M \leqslant J$ and $-J' \leqslant M' \leqslant J'$. As stated above, the amplified beam does not contain a π-polarized component. As a result, the populations of the above sublevels are no longer equal. The second group is then necessarily composed of Zeeman sublevels. The population equations associated with this group describe the variation of population of sublevels, and account for the interaction between the XRL beam and the neonlike ions. It is important to emphasize that the population equations associated with the two groups are solved simultaneously and consistently with the radiative transfer equation.

The fractional populations of the Zeeman sublevels are defined by $n_{JM}=\langle JM|\varrho|JM\rangle$, where the density-matrix operator ϱ is solution of the Bloch relation $i\hbar\partial\varrho/\partial t=[H,\varrho]$, with $H=H_A-\mathbf{d}\cdot\mathbf{E}$. The atomic Hamiltonian H_A accounts for all collisional and radiative processes, except absorption and stimulated emission. The interaction between the x-ray beam and the lasing ions is represented by $\mathbf{d}\cdot\mathbf{E}$ in the dipole approximation. The Bloch relation then yields the equations

$$\begin{aligned}\frac{\partial}{\partial t}n_{J_iM_i}(z,t)=&\,r_{J_iM_i}(t)-\Lambda_{J_iM_i}(t)n_{J_iM_i}(z,t)\\&-\sum_{q=-1,1}[n_{J_iM_i}(z,t)-n_{J'M_i-q}(z,t)]\\&\times\langle J_iM_i|d_q|J'M_i-q\rangle^2\\&\times\frac{1}{2\hbar^2\varepsilon_0 c}\int d\nu I^{(q)}_{J_iJ'}(\nu,z,t)\Phi_{J_iJ'}(\nu)\end{aligned}\tag{11}$$

for the upper sublevels, and

$$\begin{aligned}\frac{\partial}{\partial t}n_{J'M'}(z,t)=&\,r_{J'M'}(t)-\Lambda_{J'M'}(t)n_{J'M'}(z,t)\\&+\sum_{i=1}^{2}\sum_{q=-1,1}[n_{J_iM'+q}(z,t)-n_{J'M'}(z,t)]\\&\times\langle J_iM'+q|d_q|J'M'\rangle^2\\&\times\frac{1}{2\hbar^2\varepsilon_0 c}\int d\nu I^{(q)}_{J_iJ'}(\nu,z,t)\Phi_{J_iJ'}(\nu)\end{aligned}\tag{12}$$

for the lower sublevels. Λ and r are the total decay rate of a sublevel and the sum of all processes populating it (except absorption and stimulated emission), respectively. As stated above, we have two lasing transitions $J_1\rightarrow J'$ and $J_2\rightarrow J'$ sharing the same lower level J'. The population of $(J'M')$ then depends on the intensities $I^{(q)}_{J_1J'}$ and $I^{(q)}_{J_2J'}$ of the two lasing radiations.

The Einstein coefficient for stimulated emission $B_{J_iJ'}$ is given by $B_{J_iJ'}=(J_i||d||J')^2/[6\hbar^2\varepsilon_0(2J_i+1)]$. Let us set

$$\Gamma^{(q)}_{J_iJ'}(z,t)=\frac{B_{J_iJ'}}{c}\int d\nu I^{(q)}_{J_iJ'}(\nu,z,t)\Phi_{J_iJ'}(\nu).\tag{13}$$

Equations (11) and (12) determine the populations of the Zeeman sublevels, and generalize the usual system of equations which govern the evolution of the level populations. The last contribution on the right-hand side of both equations represents the effect of the x-ray beam on the sublevels populations. The line profiles $\Phi_{J_iJ'}(\nu)$ are calculated numerically by using a fast line shape code which accounts for Doppler, ion Stark, and collisional broadening effects [29]. Ion dynamics is also taken into account. It has been checked that the Stark broadening due to neighboring ions, as well as electron impact broadening, are very small for the investigated cases ($3p$-$3s$ transitions in neonlike iron).

In the absence of polarized incident radiation, we have $I^{(1)}=I^{(-1)}$. In this case, we can easily show that $n_{J_iM_i}=n_{J_i-M_i}$ and $n_{J'M'}=n_{J'-M'}$. Moreover, using the well-known property $\langle J_iM_i|d_1|J'M_i-1\rangle^2=\langle J_i-M_i|d_{-1}|J'-M_i+1\rangle^2$, and dropping the z and t coordinates for clarity, we obtain the population equations of the sublevels associated with the three lasing levels, $J_1=0$, $J_2=2$, and $J'=1$:

$$\begin{aligned}\frac{\partial}{\partial t}n_{00}&=r_{00}-\Lambda_{00}n_{00}-[n_{00}-n_{11}]2\Gamma^{(1)}_{01},\\\frac{\partial}{\partial t}n_{22}&=r_{22}-\Lambda_{22}n_{22}-[n_{22}-n_{11}]3\Gamma^{(1)}_{21},\\\frac{\partial}{\partial t}n_{21}&=r_{21}-\Lambda_{21}n_{21}-[n_{21}-n_{10}]\tfrac{3}{2}\Gamma^{(1)}_{21},\\\frac{\partial}{\partial t}n_{20}&=r_{20}-\Lambda_{20}n_{20}-[n_{20}-n_{11}]\Gamma^{(1)}_{21},\\\frac{\partial}{\partial t}n_{11}&=r_{11}-\Lambda_{11}n_{11}+[n_{22}-n_{11}]3\Gamma^{(1)}_{21}\\&\quad+[n_{20}-n_{11}]\tfrac{1}{2}\Gamma^{(1)}_{21}+[n_{00}-n_{11}]\Gamma^{(1)}_{01},\\\frac{\partial}{\partial t}n_{10}&=r_{10}-\Lambda_{10}n_{10}+[n_{21}-n_{10}]3\Gamma^{(1)}_{21}.\end{aligned}\tag{14}$$

The population equations associated with the first group, plus Eqs. (8)–(10) and (14), are solved consistently. The electron density, electron and ion temperatures, which are inputs in the MB routine, are given by EHYBRID, at the time and cell of peak gain. We have $N_e=7\times10^{20}\,\mathrm{cm}^{-3}$, $T_e=220$ eV, and $T_i=45$ eV for the first main pulse, and $N_e=6.5\times10^{20}\,\mathrm{cm}^{-3}$, $T_e=240$ eV, and $T_i=85$ eV for the second pulse. The intensity of the 0–1 line is represented as a function of the propagation length (Fig. 3). The intensity given by Linford *et al.*'s formula [24], which better fits our calculated intensity, is also represented in the small-signal

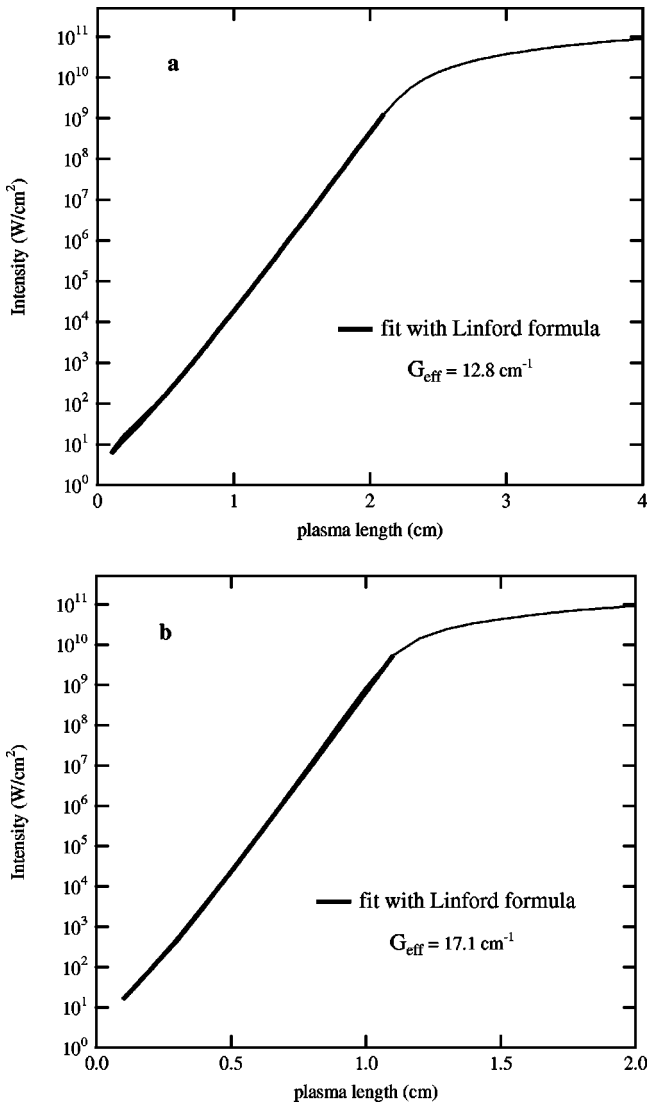

FIG. 3. Intensity of 0-1, as a function of the amplification length, at the time of peak gain for the first (a) and second (b) main pulses. We also represent the intensity given by Linford *et al.*'s formula, in the small-signal regime. G_{eff} designates the effective gain. The calculation uses a consistent Maxwell-Bloch routine, where the inputs are obtained by modeling the experiment of Zeitoun *et al.* with the EHYBRID code.

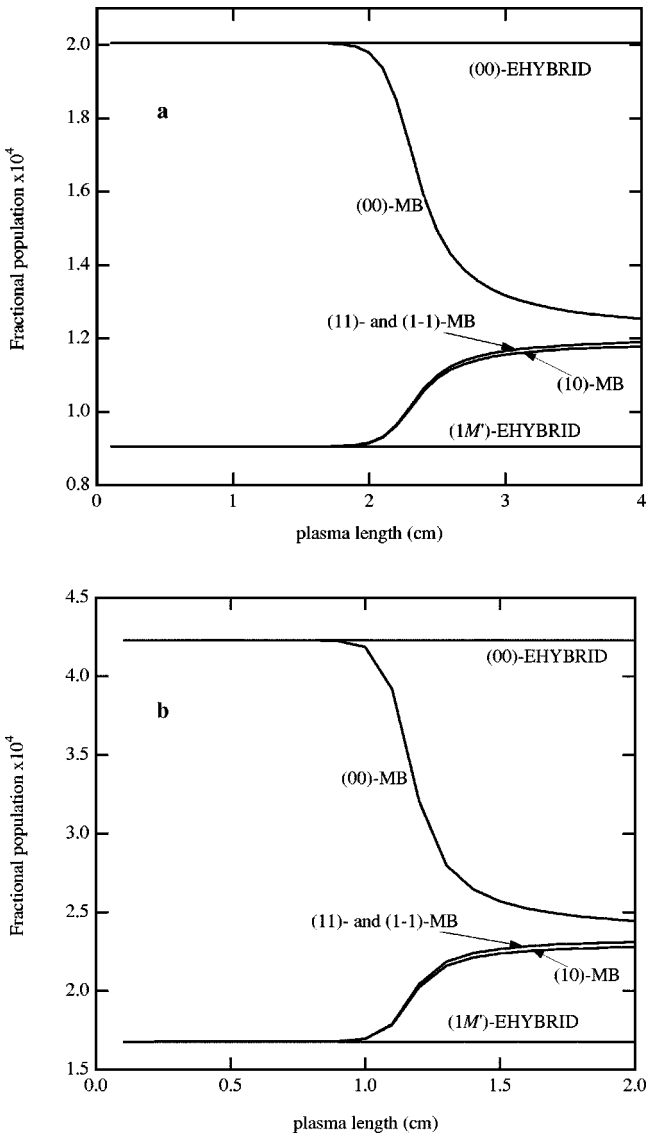

FIG. 4. Fractional population density of the Zeeman sublevels, $(1M')$ and (00), involved in the 0–1 line as a function of the amplification length, at the time of peak gain for the first (a) and second (b) main pulses. The results are obtained in the conditions of the experiment of Zeitoun *et al.*

regime. We are then able to derive an effective gain for the two main pulses (see Table I, MB row). The difference between EHYBRID and MB results is not surprising, since the former ignores the line propagation and provides a local gain. In the MB approach, the gain is defined in a similar way to experiment. The comparison to the measured gain is then meaningful. It is clear that the agreement with experimental results is better when one uses the MB routine rather than EHYBRID. One can conclude that the interaction of the XRL beam with the plasma (i) has an important effect on calculated gains as long as large intensities are involved in the fit process, and (ii) describes the saturation regime through the coupling of the radiative transfer equation with the population equations.

Figure 4 presents the fractional populations of (00) and $(1M')$. We see that the populations vary notably with z, showing the importance of the interaction between the XRL beam and the lasing ions, in the saturation regime. The absence of the π-polarized component from the amplified line is responsible for a population difference between (1 ± 1) and (10). However, elastic electron-ion collisions tend to balance the populations among the various sublevels. As a result, the population of (1 ± 1) differs by a small amount from that of (10). It is important to compare these results to the populations given by EHYBRID. For this purpose, we assume that the $J'=1$ level population given by EHYBRID is equally distributed among the three Zeeman sublevels. This is a rigorous assumption, since the above model does not account for any mechanism unbalancing the sublevel populations. We also plot these fractional populations. For z

TABLE II. The rates $\Gamma_{01}^{(1)}$, C_{01}, and A_{01} are given (in s^{-1}) for the two main pulses. $\Gamma_{01}^{(1)}$ is calculated for an amplification length of 2.1 cm (first pulse) or 1.1 cm (second pulse).

	First pulse	Second pulse
Amplification length	2.1	1.1
Γ_{01}	2.24×10^{11}	4.18×10^{11}
A_{01}	4.77×10^{9}	4.77×10^{9}
C_{01}	5.12×10^{11}	4.24×10^{11}

$<z_{sat}$, where $z_{sat}=2$ cm for the first pulse and 1 cm for the second, the magnitude of the XRL intensity is such that the rates $\Gamma_{J_iJ'}^{(1)}$ [see Eq. (13)] remain small and cannot yield a significant effect on populations. As the MB routine is essentially based on the EHYBRID code, the two calculations give identical populations, for small XRL intensities. For larger z values, the effect of the XRL beam becomes important. In fact, for an elementary lasing transition, $(00)\rightarrow(1\pm1)$, the rate $\Gamma_{01}^{(1)}$ is of the same order of magnitude at the collisional deexcitation rate C_{01} but is much larger than the spontaneous emission rate A_{01} (see Table II). As a result, the $J_1=0$ level is considerably depleted, while the $(1M')$ populations increase by a large amount, yielding local gains that are smaller than those given by EHYBRID for the two elementary lasing transitions.

IV. CONCLUSIONS

We have modeled an experiment on the neonlike iron x-ray laser by using the EHYBRID code. This code does not account for the interaction between the x-ray beam and the plasma, and yields much larger gains than actually measured. A more complete approach combining the Maxwell wave equation and the Bloch relation yields a set of population equations containing a contribution that is due to stimulated emission and absorption. This set, which involves the three lasing levels $J_1=0$, $J_2=2$, and $J'=1$ only, governs the evolution of the populations of the sublevels (00), $(2M)$, and $(1M')$. It is completed by population equations for all other neonlike levels. The ensemble of equations is solved consistently with the radiative transfer equation. As the 2–1 line shares the same lower level with the 0–1 line the population of (00) depends on the populations of $(2M)$. For this reason, our calculations for the 0–1 line also accounts for the 2–1 line, despite the fact that we were not interested in the output of the 2–1 line. We have calculated the intensity of the XRL beam vs the amplification length, and an effective gain was derived by using Linford *et al.*'s formula, in the small-signal regime. We have obtained, for the 0–1 line, an effective gain, in better agreement with experiment than the gain given by EHYBRID. We have also investigated the variation with the amplification length of the fractional populations n_{00} and $n_{1M'}$. The intensity of the 2–1 line is very small, in comparison to the intensity of the 0–1 line. As a consequence, the populations of $(2M)$ (not presented) do not vary with z.

[1] D. L. Matthews, P. L. Hagelstein, M. D. Rosen, M. J. Eckart, N. M. Ceglio, A. Hazi, H. Medecki, B. J. MacGowan, J. E. Trebes, B. L. Whitten, E. M. Campbell, C. W. Hatcher, A. M. Hawryluk, R. L. Kauffman, L. D. Pleasance, G. Rambach, G. H. Scofield, G. Stone, and T. Weaver, Phys. Rev. Lett. **54**, 110 (1985).

[2] B. Rus, A. Carillon, P. Dhez, P. Jaeglé, G. Jamelot, A. Klisnick, M. Nantel, and P. Zeitoun, Phys. Rev. A **55**, 3858 (1997).

[3] J. Zhang, A. G. MacPhee, J. L. J. Nilsen, J. Lin, T. W. Barbee, Jr., C. Danson, M. H. Key, C. L. S. Lewis, D. Neely, R. M. N. O'Rourke, G. J. Pert, R. Smith, G. J. Tallents, J. S. Wark, and E. Wolfrum, Phys. Rev. Lett. **78**, 3856 (1997).

[4] J. Zhang, A. G. MacPhee, J. Lin, E. Wolfrum, R. Smith, C. N. Danson, M. H. Key, C. L. S. Lewis, D. Neely, J. Nilsen, G. J. Pert, G. J. Tallents, and J. S. Wark, Science **276**, 1097 (1997).

[5] S. Sebban, H. Daido, N. Sakaya, Y. Kato, K. Murai, H. Tang, Y. Gu, G. Huang, S. Wang, A. Klisnick, Ph. Zeitoun, F. Koike, and H. Takenaka, Phys. Rev. A **61**, 43 810 (2000).

[6] P. Lu, H. Nakano, T. Nishikawa, and N. Uesugi, Proc. SPIE **3886**, 294 (2000).

[7] Y. Li, P. Lu, G. Pretzler, and E. E. Fill, Opt. Commun. **133**, 196 (1997).

[8] B. J. MacGowan, L. B. DaSilva, D. J. Fields, C. J. Keane, J. A. Koch, R. A. London, D. L. Matthews, S. Maxon, S. Mrowka, A. L. Osterheld, J. H. Scofield, G. Shimkaveg, J. E. Trebes, and R. S. Walling, Phys. Fluids B **4**, 2326 (1992).

[9] J. J. Rocca, D. P. Clark, F. G. Tomasel, V. N. Shlyaptsev, J. L. A. Chilla, B. Benware, C. Moreno, D. Burd, and J. J. Gonzalez, in *Proceedings of the Sixth International Conference on X-ray Lasers*, edited by Y. Kato, H. Takuma, and H. Daido, IOP Conf. Proc. No. 159 (Institute of Physics and Physical Society, London, 1998), p. 9.

[10] A. Carillon, H. Z. Chen, P. Dhez, L. Dwivedi, J. Jacoby, P. Jaeglé, G. Jamelot, J. Zhang, M. H. Key, A. Kidd, A. Klisnick, R. Kodama, J. Krishnan, C. L. S. Lewis, D. Neely, P. Norreys, D. O'Neill, G. J. Pert, S. A. Ramsden, J. P. Raucourt, G. J. Tallents, and J. Uhomoibhi, Phys. Rev. Lett. **68**, 2917 (1992).

[11] J. Zhang, P. J. Warwick, E. Wolfrum, M. H. Key, C. Danson, A. Demir, S. Healy, D. H. Kalantar, N. S. Kim, C. L. S. Lewis, J. Lin, A. G. MacPhee, D. Neely, J. Nilsen, G. J. Pert, R. Smith, G. J. Tallents, and J. S. Wark, Phys. Rev. A **54**, R4653 (1996).

[12] G. M. Shimkaveg, M. R. Carter, R. S. Walling, J. M. Ticehurst, R. A. London, R. E. Stewart, in *Proceedings of the Third International Conference on X-ray Lasers*, edited by E. E. Fill, IOP, Conf. Proc. No. 125 (Institute of Physics and Physical Society, London, 1992), p. 61.

[13] J. E. Balmer, R. Tommasini, and F. Lowenthal, IEEE J. Sel. Top. Quantum Electron. **5**, 1435 (1999).

[14] P. Zeitoun, A. MacPhee, F. Albert, A. Carillon, P. Jaeglé, G. Jamelot, A. Klisnick, M. Maillard, D. Ros, B. Rus, S. Sebban, C. L. S. Lewis, N. O'Rourke, J. Warwick, R. Smith, and G. J. Tallents, in *Proceedings of the Sixth International Conference on X-ray Lasers* (Ref. [9]), p. 115.

[15] J. Nilsen, B. J. MacGowan, L. B. Da Silva, and J. C. Moreno, Phys. Rev. A **48**, 4682 (1993).
[16] G. J. Pert, J. Comput. Phys. **39**, 251 (1980).
[17] P. B. Holden, S. B. Healy, M. T. M. Lightbody, G. J. Pert, J. A. Plowes, A. E. Kingston, E. Robertson, C. L. S. Lewis, and D. Neely, J. Phys. B **27**, 341 (1994).
[18] E. A. Watson, H. M. Gibbs, F. P. Mattar, M. Cormier, Y. Claude, S. L. McCall, and M. S. Feld, Phys. Rev. A **27**, 1427 (1983).
[19] A. Crubellier, S. Liberman, and P. Pillet, J. Phys. B **19**, 2959 (1986).
[20] G. Hazak and A. Bar-Shalom, Phys. Rev. A **38**, 1300 (1988).
[21] M. Strauss, Phys. Fluids B **1**, 907 (1989).
[22] R. A. London, M. Strauss, and M. D. Rosen, Phys. Rev. Lett. **65**, 563 (1990).
[23] H. R. Griem, *Plasma Spectroscopy* (McGraw-Hill, New York, 1964).
[24] G. J. Linford, E. R. Peressini, W. R. Sooy, and M. L. Spaeth, Appl. Opt. **13**, 379 (1974).
[25] R. A. London, Phys. Fluids **31**, 184 (1988).
[26] B. Rus, P. Zeitoun, T. Mocek, S. Sebban, M. Kálal, A. Demir, G. Jamelot, A. Klisnick, B. Králiková, J. Skála, and G. J. Tallents, Phys. Rev. A **56**, 4229 (1997).
[27] A. Sureau and P. B. Holden, Phys. Rev. A **52**, 3110 (1995).
[28] D. Benredjem, A. Sureau, and C. Möller, Phys. Rev. A **55**, 4576 (1997).
[29] B. Talin, A. Calisti, L. Godbert, R. Stamm, R. W. Lee, and L. Klein, Phys. Rev. A **51**, 1918 (1995).